Towards a novel *in vivo* model of Parkinson's disease: Mitochondrial targeted α-synuclein overexpression in rats

A. Leonte

(s2298104)

September 2017

Minor Thesis, MRes Behavioural and Cognitive Neurosciences

Faculty of Science and Engineering

University of Groningen

Supervised by: Dr. A. S. Boerema & Prof. dr. U. L. M. Eisel

Abstract

Parkinson's disease (PD) is associated with the accumulation of abnormal α-synuclein (α-syn) causing loss of dopaminergic neurons in the substantia nigra (SN). This translates to a progressive decline in striatal dopamine and associated motor deficits. The mechanisms underlying α-syn neurotoxicity are not completely understood, but evidence suggests prominent roles for mitochondrial dysfunction and neuroinflammation in PD pathogenesis. To study the interaction between both components and their role in α-syn neurotoxicity, we aimed to develop a novel disease model that incorporates the two mechanisms. In this within-subjects study, we compare the effects of cytosolic targeting and mitochondrial targeting of α-syn overexpression in the SN of rats using adeno-associated viral vectors (AAV2). Neuroinflammation and dopaminergic neurodegeneration were monitored longitudinally using ^{11}C-PBR28 and ^{18}F-FDOPA Positron Emission Tomography (PET) imaging, and behavioural testing for motor symptoms. Results indicated a striking absence of dopaminergic neurodegeneration and decline in motor performance. In contrast, VOI analyses showed a robust increase in neuroinflammation three and six weeks following cytosolic as well as mitochondrial targeted α-syn overexpression. Although no differences between cytosolic and mitochondrial targeting were found, microglia activation was successfully manipulated when α-syn was overexpressed. Further histological investigations need to be performed in order to elucidate the role of a-syn accumulation in neuroinflammation. The missing pattern of dopaminergic neurodegeneration could be explained by issues within the experimental design, or by the need of a larger time span for the development of dopamine related symptoms.

Keywords: Parkinson's disease, α-synuclein, adeno-associated virus, mitochondrial dysfunction, neuroinflammation, longitudinal PET-imaging

Towards a novel *in vivo* model of Parkinson's disease: Mitochondrial targeted α-synuclein overexpression in rats

The epidemic of neurodegenerative diseases represents the paradoxical consequence of mankind's strive for a prolonged lifespan. Parkinson's disease (PD) forms part of a spectrum of neurodegenerative diseases collectively termed synucleinopathies. The pathological accumulation of the protein α-synuclein (α-syn) especially is neurotoxic to dopamine producing neurons in the substantia nigra pars compacta (SN). Dopaminergic cell death leads to a progressive decrease in nigrostriatal dopamine, the main neurotransmitter involved in motor control. PD clinically manifests as motor dysfunctions including resting tremor, rigidity, and gait disturbances (Dauer & Przedborski, 2003). Early appearing non-motor symptoms include impaired olfaction and gastrointestinal problems. Advanced stages of the disease are commonly associated with cognitive impairment proceeding to dementia in some cases, mood disturbances and emotional disturbances (Dauer & Przedborski, 2003). The specific symptomatic profile implicates the propagation of PD pathology, originating at a site other than the CNS. Indeed, Braak and his colleagues (2003) hypothesize a staged development of PD whereby α-syn aggregation first emerges in the gastrointestinal tract (Braak et al., 2006) and ascends via the vagus nerve to the lower brain stem (Holmqvist et al., 2014), reaching the basal mid-and forebrain, and extending to the neocortex. In line with this, α-syn aggregates have been shown to propagate through neural networks via cell-to-cell transmission in a prion-like manner (Bernis et al., 2015) enabling them to affect widespread regions in the brain.

α-Syn is highly present within the brain, representing about 1% of the total brain protein (Campbell et al., 2000). The physiological role of α-syn however, is not completely understood. A large number of studies suggests its primary localization at the synapse. The small, and highly mobile protein is thought to play a role in synaptic plasticity, and to interact – though only weakly – with cellular membranes (Bendor et al., 2013). The protein's native structure exists as monomers or tetramers. Under disease conditions α-syn undergoes conformational change presumably due to post-translational modifications of the protein (Rockenstein et al., 2014), point mutations (A53T and A30P) (Polymeropoulos et al., 1997; Kruger et al., 1998) or duplications and triplications (Ibanez et al., 2004; Singleton et al., 2003) of the α-syn encoding gene, *SNCA.* Misfolded α-syn makes the protein more insoluble resulting in an accumulation of the aggregates which form the primary structural components of Lewy bodies often found in PD (Spillantini et al., 1997). However, neurotoxicity in PD is thought to mainly derive from aggregated α-syn fibrils termed Lewy neurites. In line with the

protein's presumed role in vesicular transport (Bendor et al., 2013), α-syn aggregates in PD are prevalent in presynaptic terminals of dopaminergic neurons in the SN (Spinelli et al., 2014) extending their toxicity along the nigrostriatal pathway. Bernheimer et al. (1973) state that the degree of terminal loss in the striatum appears to be more pronounced than the magnitude of dopaminergic cell loss in the SN. Thus, abnormal α-syn accumulation seems to primarily affect nerve terminals.

By a still unknown mechanism, α-syn aggregates impair a variety of cellular processes ultimately leading to the death of the cell. A large body of evidence suggests that chronic inflammation in the brain may enhance the protein's toxic effects by adding fuel to the fire (Reish & Standaert, 2015). Indeed, PD pathology seems to involve innate as well as adaptive immune system activation (Taylor et al., 2013; Bartels et al., 2010). Upon extracellular release from affected cells, α-syn aggregates may serve as a pathological trigger for an inflammatory response driven by the CNS resident immune cells termed microglia. This is supported by the finding that microglia activation positively correlates with α-syn load in post-mortem brains of PD patients (Croisier et al., 2005). By secreting pro-inflammatory cytokines and chemokines, activated microglia initiate tissue repair and clearance of debris. Elevated levels of pro-inflammatory mediators secreted by microglia such as tumor necrosis factor-α (TNF-α), interleukin-1β (IL-1β), IL-6 and interferon-γ (IFN-γ) have been found in post-mortem brains and cerebrospinal fluid of PD patients (Reish & Standaert, 2015). Besides correlational evidence, Sanchez-Guajardo and her colleagues (2010) demonstrated that α-syn drives the inflammatory response directly. The authors found differences in the degree and type of immune response when manipulating α-syn expression levels using a viral vector model. While inflammatory responses instigate the healing process, consecutive inflammation may disturb tissue homeostasis. Chronic high levels of pro-inflammatory elements compromise the permeability of the blood brain barrier (BBB) and promote the infiltration of T- and B- lymphocytes in the normally immune privileged brain. In addition, prolonged inflammation generates persistent high levels of free radicals released by activated microglia (Dheen et al., 2007). When phagocytosed, aggregated α-syn seems to upregulate the production and release of reactive oxygen species (ROS) by microglia (Zhang et al., 2005). Taken together, subsequent microglia activation due to pathogenic α-syn aggregation and accumulation leads to an elevation of pro-inflammatory elements resulting in a "leaky" BBB, the recruitment of peripheral leukocytes, and the generation of toxic reactive species. According to Gao et al. (2008), inflammatory-derived ROS affect α-syn's conformation in an unfavourable manner stimulating α-syn aggregation. Thus, the affected brain region resides in

a robust inflammatory condition which is maintained due to the continuous presence of α-syn aggregates.

Next to inflammatory-derived reactive species, PD pathology is thought to involve mitochondrial impairment. Evidence of mitochondrial dysfunctions in PD first came from studies in which a link between mitochondria affecting toxins such as 1-methyl-4-phenyl-1,2,3,6-tetrahydrodropyridine (MPTP) and a Parkinsonian behavioural phenotype was established (Langston et al., 1983; Burns et al., 1985). In a similar vein, the mitochondrial complex I inhibitor, rotenone, leads to a robust parkinsonian phenotype (Cannon et al., 2009). Impaired mitochondrial complex I activity in the SN represents a probable cause of increasing intracellular levels of ROS in PD (Beal, 2003). In line with this, scientists have found a significant complex I deficiency in post-mortem brains of PD patients (Schapira et al., 1990; Schapira et al., 2007), and α-syn aggregation affecting mitochondrial function *in vitro* (Hsu et al., 2000). Although being a normal byproduct of the electron transport chain, ROS can inflict oxidative damage to adjacent biomolecules (e.g. DNA, proteins, membrane lipids) essential for the functionality of the neuron. Impaired mitochondrial functioning may disturb the energy production process and promote the release of free radicals to the cytosol thereby creating a cytotoxic environment termed oxidative stress. The resulting oxidative stress has been implicated in several neurodegenerative diseases (Li et al., 2013). This can be attributed, in part, to the finding that oxidative stress can affect protein conformation. Indeed, α-syn aggregation in PD may be enhanced when mitochondrial functioning is impaired (Giasson et al., 2000). Furthermore, the considerable amounts of ROS produced due to complex I deficits promote mitochondrial cytochrome c release to the cytosol (Perier et al., 2005), an event likely to stimulate pro-apoptotic pathways. This is confirmed by Parihar et al. (2008) who have shown that α-syn oligomers bind to the mitochondrial membrane. As a consequence, cytochrome c is released from the mitochondria thereby increasing intracellular oxidative stress (Parihar et al., 2009). When functionality of the mitochondrial complex I is compromised, dopaminergic neurons in the nigrostriatal pathway seem to be more susceptible to exogeneous parkinsonian neurotoxins (Perier et al. 2010). In the same way, when catalases in the mitochondria are highly expressed, dopaminergic neuroprotection against mitochondria-derived ROS is ensured. Also, α-syn overexpression positively correlates with MPTP susceptibility while α-syn absence seems to be neuroprotective for the same toxin (Thomas & Beal 2007; Dauer et al., 2002) providing support for mitochondrial involvement in dopaminergic neurodegeneration due to α-syn toxicity. Taken together, α-syn aggregates presumably disrupt mitochondrial oxidative metabolism by inhibiting complex I activation

thereby increasing ROS production and cytosolic cytochrome c release. As a result, the cytotoxic environment and subsequent stimulation of pro-apoptotic events is maintained winding up in a downwards spiral of dopaminergic neurodegeneration.

The indisputable evidence that both mechanisms – chronic inflammation in the brain and mitochondrial dysfunctions – form important contributors to PD pathology now needs to be incorporated into a comprehensive disease model. In this way, disease development, possibilities for preventive and neuroprotective interventions can be studied more accurately. Valuable insights into neuropathological mechanisms have come from studies using transgenic mice (Tg) which overexpress wild-type (WT) or point mutated (human) α-syn. Equivalent to human disease conditions, overexpression of α-syn in Tg mice is related to low levels of nigrostriatal dopamine. In addition, genetic modified mice show mitochondrial dysfunctions and oxidative stress, two evidence-based components of PD pathophysiology (Bender et al., 2013). Using these models, scientists have been able to partly elucidate molecular pathways responsible for dopaminergic neurodegeneration providing a platform for innovative drug development. However, a common critic of Tg mouse models is the clear presence of actual dopaminergic cell death overtime despite the presence of high α-syn levels (Matsuoka et al., 2001; Visanji et al., 2016). Low transgenic expression levels, the fact that α-syn is overexpressed since embryonic stages and/or the absence of a disease-specific trigger serve as possible explanations for the Tg models' limitations. In addition, genetic mutations are primarily associated with inherited cases of PD and therefore not suited to study sporadic PD.

As previously discussed, toxin based models nicely demonstrate the likely role of mitochondrial dysfunctions in PD. As such, they have been widely used by scientists to study neuroprotective pathways in dopaminergic neurodegeneration. Apart from the leading MPTP and rotenone models, the use of the 6-hydroxydopamine (6-OHDA) is extensive. Introduced by Ungerstedt (1968), the 6-OHDA lesion model is efficient and effective due to its preferential uptake by dopamine producing neurons. 6-OHDA is also associated with cytosolic accumulation leading to increasing ROS levels. However, the missing activation of programmed cell death pathways in the 6-OHDA lesion model (Jeon et al., 1995) makes it less attractive to study PD pathogenesis since pro-apoptotic events are likely (Visanji et al., 2016). Furthermore, the 6-OHDA model does not incorporate the time-dependent degeneration of dopamine neurons characteristic for PD (Jeon et al., 1995), and is usually not associated with Lewy body formation making it unsuitable to study the temporal dynamics of α-syn toxicity.

Promising novel technologies to deliver genetic material at a certain point in time *in vivo* have evolved over the past few years and shown promising results in mirroring human parkinsonism. Adeno-associated viruses (AAV), belonging to the family of *Parvoviridae,* and incorporating the human α-syn transgene are directly delivered to a specific site. AAVs enabled scientists to overexpress α-syn and mimick the temporal expression of Parkinson-related motor deficits, the presence of α-syn inclusions and dopaminergic neurodegeneration in the nigrostriatal tract (Kirik et al., 2002; Decressac et al., 2012; Decressac et al., 2011). Injecting a recombinant type of the AAV vector directly into the SN of rats, Van der Perren and her co-workers (2015) have demonstrated the model's ability to cause dopaminergic neurodegeneration. Using non-invasive neuroimaging, the authors found a time-dependent decrease in dopamine, but also a decline in dopamine-related motor performance and the cumulative accumulation of α-syn positive aggregates. However, the authors' results mostly relate to familial PD as they have overexpressed A53T, a mutant type of α-syn which is not necessarily the reason for the development of sporadic PD. Decressac et al. (2012) introduced an AAV model to overexpress human WT α-syn, a study on which the present research is largely based. The authors aimed to maximize viral transduction efficiency by overexpressing human wildtype α-syn downstream of a synapsin 1 promoter, a gene promoter associated with a high tropism for neurons and long-term transgene expression *in vivo* (Kügler et al., 2003). Furthermore, introducing a woodchuck hepatitis virus post-transcriptional regulatory element (WPRE) enhances and ensures long-term transgene expression. In this way, α-syn containing vector injections yielded a substantial loss of TH (tyrosine hydroxylase) – the enzyme responsible for the production of the dopamine precursors – positive cells compared to a control vector in which α-syn was substituted for eGFP. Viral expression was largely confined to the SN highlighting the degree of tropism of the viral vector. The loss of striatal TH positive fibers implicates that nigral injection of the virus is associated with a striatal extension of α-syn toxicity. The described neuropathology significantly correlated with the decline in dopamine-related motor performance.

Inspired by Decressac et al.'s (2012) methodology, the present study aims to integrate recent evidence of mitochondrial dysfunctions due to α-syn and propose a novel *in vivo* model for PD. Here, we want to show that targeting the mitochondria with α-syn overexpression will lead to a more aggressive progression of neuropathology and behavioural symptomatology as compared to standard cytosolic targeting. Preliminary *in vitro* results indicate that mitochondrial targeting of α-syn overexpression leads to a higher loss of dopaminergic neurons compared to cytosolic targeting of α-syn overexpression in cell culture experiments.

Aiming to validate these results *in vivo*, the current study makes use of longitudinal positron emission tomography (PET) imaging and behavioural testing to allow for comprehensive inferences about the viruses' effects.

Materials & Methods

Animals

Sixteen adult female Sprague Dawley rats, 225–250 g at the time of surgery, were housed in individually ventilated cages with *ad libitum* access to food and water during a 12 h light/dark cycle. After arrival, animals were allowed to acclimatize for at least 7 days. All procedures except PET imaging were conducted at the appropriate containment level. The study was conducted in accordance with the ethical guidelines of, and approved by the Institutional Animal Care and Use Committee of the University of Groningen under license number DEC-5902O.

Study design

Half of the rats were randomly allocated to receive the mitochondrial targeting virus while the other half received the cytosolic targeting vector. Baseline measurements were performed 1-5 days prior to viral injections. All animals were followed longitudinally using non-invasive dopaminergic and neuroinflammatory PET-imaging, and behavioural examination. Viral expression is thought to be abundant 14 days following injections *(Ganjam & Culmsee, personal communication)*. Time points for PET scans and behavioural experiments were selected on week 3 and week 6 after viral injections. Time points were limited to an interval of 3 weeks due to ethical and practical considerations.

Viruses

Four different vector constructs were used to compare mitochondrial to cytosolic targeted overexpression of human WT α-syn: (1) the AAV2-αSYN vector (2.83×10^9 TU/µl) and (2) the control AAV2-eGFP vector (4.73×10^9 TU/µl), (3) the AAV2-MTS-αSYN (5.72×10^9 TU/µl) and (4) the AAV2-MTS-eGFP (3.45×10^7 TU/µl). The two latter vectors included a mitochondrial targeting signal upstream of the α-syn ecoding gene. All four viral vectors included the synapsin-1 gene promoter upstream of the transgene to ensure high transcription rates. Expression of the transgene was enhanced using a WPRE and viral vectors were provided by Dr. G. K. Ganjam (Dr. Culmsee group, Philipps University of Marburg). A detailed description of the viruses can be found in the appendix. Cell culture experiments performed by the same group showed that AAV2-αSYN as well as AAV2-MTS-αSYN infection were associated with a significant amount of dopaminergic cell death in contrast to

the eGFP vector variants. Furthermore, cell viability in mitochondrial targeted cultures exhibited an almost 40% drop compared to cytosolic targeted neurons.

Surgical procedures

All surgical procedures were performed under general anesthesia (2.5 % isoflurane). Rats were placed in a stereotaxic frame (Kopf) and vector solutions were injected using a 10 µl Hamilton syringe equipped with a 31 Ga steel needle. Similar to previous studies (e.g., Decressac et al., 2012), 3 µl of vector solution was injected at a rate of 0.2 µl/min bilaterally with either the AAV2-αSYN (right hemisphere) and the respective control vector AAV2-eGFP (left hemisphere), or the AAV2-MTS-αSYN (right hemisphere) and the respective control vector AAV2-MTS-eGFP (left hemisphere) above the SN at the following coordinates (flat skull position) relative to Bregma: anteroposterior at -5.3 mm, mediolateral at -2.2 mm and dorsoventral at -7.8 mm. The needle was left in place for an additional 5 min period before it was slowly retracted. Three animals died during surgery leaving six rats that received the cytosolic targeting vectors while seven rats received the novel mitochondrial targeting vector. A detailed overview of the injections is provided in the appendix.

Small animal PET-image acquisition

Functional dopamine activity. PET imaging can detect impairment of functional dopamine activity in the living brain using the radioactive tracer l-3,4-dihydroxy-6-[^{18}F]fluoro-phenylalanine (^{18}F-FDOPA), a fluorinated positron-emitting equivalent of the neurotransmitter's immediate precursor L-DOPA (Kyono et al., 2011). ^{18}F-FDOPA levels positively correlates with dopamine metabolism and vesicular uptake in the nigrostriatal presynaptic nerve terminals. Low ^{18}F-FDOPA uptake is associated with a high degree of dopamine-related motor deficits such as in PD (Kyono et al., 2011).

Dopaminergic PET-imaging was performed at the University Medical Center of Groningen in a dedicated small animal Siemens/Concorde Focus 220 scanner. Aneasthesia was induced by 5% isoflurane in oxygen enriched (60%) air and maintained with 2% isoflurane inhalation. Rats were kept on heating pads at all times to maintain body temperature, eye salve was applied onto the eyes to prevent dehydration, and tail vein cannulations were administered. The protocol for peripheral ^{18}F-FDOPA uptake blockade was adapted from Walker et al. 2013 and based on pilot studies. A combination of 1 ml of Benserazide (10 mg/ml) + Entacapone (1 mg/ml) in PBS was intravenous (iv) injected via the cannula 35 minutes before tracer injection. An additional 0.125 ml of Entacapone (25 mg/ml in DMSO) was intraperitoneally injected 30 minutes before tracer injection to ensure full blockade. Animals were then placed on the PET scanner bed (max 4 animals per scan) in

prone position and the heads in the field of view. Radioactive ^{18}F-FDOPA tracer (32 ± 8 MBq in ~1 ml of saline solution) was administered over a 1-min period via the tail vein cannula which was then flushed with a saline-heparin solution (0.25 ml). A transmission scan of 10 minutes with a ^{57}Co point source was performed for attenuation, scatter and random coincidences, and decay of radioactivity. Body temperature, heart rate and blood oxygenation level were monitored throughout the duration of the scans. After scanning, animals were put on 100% oxygen and kept warm on heating pads.

Microglia activation. The PET ligand *N*-acetyl-*N*-(2-[^{11}C]methoxybenzyl)-2-phenoxy-5-pyridinamine (^{11}C-PBR28) developed by Imaizumi et al. (2008) serves as a suitable imaging tool to estimate the amount of neuroinflammation. The ligand binds to peripheral benzodiazepine receptors (PBR) that are upregulated on activated microglia. ^{11}C-PBR28 uptake thus serves as an estimation of the amount of neuroinflammation.

PET imaging was performed at the University Medical Center of Groningen in a dedicated small animal Siemens/Concorde Focus 220 scanner. Aneasthesia was induced by 5% isoflurane in oxygen enriched (60%) air and maintained with 2% isoflurane inhalation. Rats were kept on heating pads at all times to maintain body temperature, eye salve was applied onto the eyes to prevent dehydration, and tail vein cannulations were administered. Animals received the radioactive tracer ^{11}C-PBR28 (50 ± 21 in ~1 ml saline solution) over a 1-min period and were flushed with a saline-heparin solution (0.25 ml) via the tail vein cannula after which static image acquisition started. A transmission scan of 10 minutes with a ^{57}Co point source was performed for attenuation, scatter and random coincidences, and decay of radioactivity. Body temperature, heart rate and blood oxygenation level were monitored throughout the duration of the scans. After scanning, animals were put on 100% oxygen and kept warm on heating pads.

Image reconstruction and analysis

^{18}F-FDOPA. List-mode data of the ^{18}F-FDOPA PET scans was separated into 2 frames (1 × 60, 1 × 40 min). Emission sinograms were normalized and corrected for attenuation, scatter and decay using the transmission data. They were then iteratively reconstructed using OSEM2D (4 iterations and 16 subsets). Final images had a 256x256x95 matrix with a pixel width of 0.815 mm and a slice thickness of 0.796 mm. Only the second frame was analyzed using several software packages. Amide (Loening & Ghambir, 2003) was used for cropping individual animals, calculation of percent injected dose (% ID), and to prepare for further image processing. Voxel size was decided to be 0.2 mm. An average template of all baseline scans was constructed using the SAMIT toolbox (Garcia et al., 2015)

that runs in SPM (MATLAB). Co-registration of individual images to the average template was done in PMod. Volumes of interests (VOIs) for the striatum (left and right) (a volume of 0.04428 cm^3 for each) and the cerebellum (volume of 0.0419 cm^3) were manually defined on the template, using the threshold function of PMod. These VOI's were re-used on the individual images, but were individually positioned. The cerebellum was used as a reference and subtracted from striatal VOIs to eliminate background noise. Resulting striatal VOI statistics were analyzed in SPSS.

^{11}C-PBR28. List-mode data of the ^{11}C-PBR28 PET scans was separated into 2 frames (1 × 45, 1 × 30 min). Emission sinograms were normalized and corrected for attenuation, scatter and decay using the transmission data. They were then iteratively reconstructed using OSEM2D (4 iterations and 16 subsets). Final images had a 256x256x95 matrix with a pixel width of 0.815 mm and a slice thickness of 0.796 mm. Only the second frame was analyzed using several software packages. Amide (Loening & Ghambir, 2003) was used for cropping individual animals, calculation of standard uptake values (SUVs), and to prepare for further image processing. Voxel size was decided to be 0.2 mm. Vinci 4.72 software (Max Planck Institute for Neurological Research, Germany) was used for manual co-registration to a PBR28 specific tracer template for Wistar rats previously created in the NGMB department (Vállez Garcia et al., 2015), coregistered to the Schwarz MRI atlas (Schwarz et al., 2006) and subsequent VOI analysis. Statistical significance testing of striatal SUVs was performed in SPSS.

The standard uptake value (SUV) of the ^{11}C-PBR28 radioactive tracer has been shown to be a valid and reliable outcome measure to infer inflammation in the rat brain (Tóth et al., 2015). SUVs per voxel were averaged for pre-determined brain regions (Schwarz et al, 2006). Striatal SUVs were calculated as the average of the caudate putamen, nucleus accumbens core and nucleus accumbens shell.

Behavioural testing

Cylinder test. To examine impaired spontaneous forelimb activity, animals were put in a glass cylinder (18 cm diameter, 30 cm height) for 5 minutes. To avoid provocation or inhibition of the rats' movement, no (excessive) sounds or movements were initiated. Rats naturally explore the cylinder by standing upwards, leaning against and moving alongside the glass wall. Placing a mirror behind the cylinder at an angle of 120 degrees enabled better visualization of forelimb activity which was recorded on camera. The first 20 forepaw touches were counted and scored as either right or left paw touches. As previous literature (Decressac

et al., 2012, Van der Perren et al., 2015), percentage of impaired forelimb activity was determined by dividing the number of left forepaw touches with the total number of touches.

Statistical Analyses

Statistical testing was conducted with IBM SPSS Statistics 21 (SPSS Inc. Chicago, The United States). Extracted mean values from the tomographic images were analyzed using a three-way repeated measures analysis of variance (RM-ANOVA) with time and hemisphere as within-subjects factors and virus (i.e., mitochondrial vs. cytosolic targeting vector) as a between-subjects factor. Behavioural data were recoded into percentages of impaired forelimb use which were then analyzed with a two-way RM-ANOVA with time as a within-subjects factor and the viral construct as a between-subjects factor. The F-test was used to report the *p*-values, which were considered statistically significant for $p<0.05$.

Results

^{18}F-FDOPA PET-imaging

On average, ^{18}F-FDOPA levels slightly decreased for the control as well as the a-syn viruses 3 weeks following injection and returned to baseline levels at week 6. Temporal changes in striatal ^{18}F-FDOPA levels however, were not statistically significant, $F(2,22) = 2.31$, $p = .12$ (Fig. 1). With a same difference of .02 % ID at week 3 (.25 ± .04 vs. .23 ± .05) and week 6 (.3 ± .06 vs. .28 ± .09), ^{18}F-FDOPA levels did not statistically differ between the cytosolic and mitochondrial targeting a-syn vector, $F(2,22) = .17$, $p = .85$ (Fig. 1B). Differences between the control virus and the a-syn virus were minimal for the cytosolic as well as the mitochondrial targeting vectors at week 3 and week 6 with $F(2,22) = 1.25$, $p = .31$ (Fig. 1A).

Table 1: *Mean (% ID) and standard deviation of striatal ^{18}F-FDOPA levels by virus and timepoint.*

Virus	Pre-injection	Week 3	Week 6
AAV2-MTS-eGFP	.29 (SD .05)	.24 (SD .03)	.28 (SD .06)
AAV2-MTS-aSYN	.28 (SD .05)	.25 (SD .04)	.3 (SD .06)
AAV2-eGFP	.26 (SD .09)	.23 (SD .07)	.3 (SD .08)
AAV2-aSYN	.25 (SD .09)	.23 (SD .05)	.28 (SD .09)

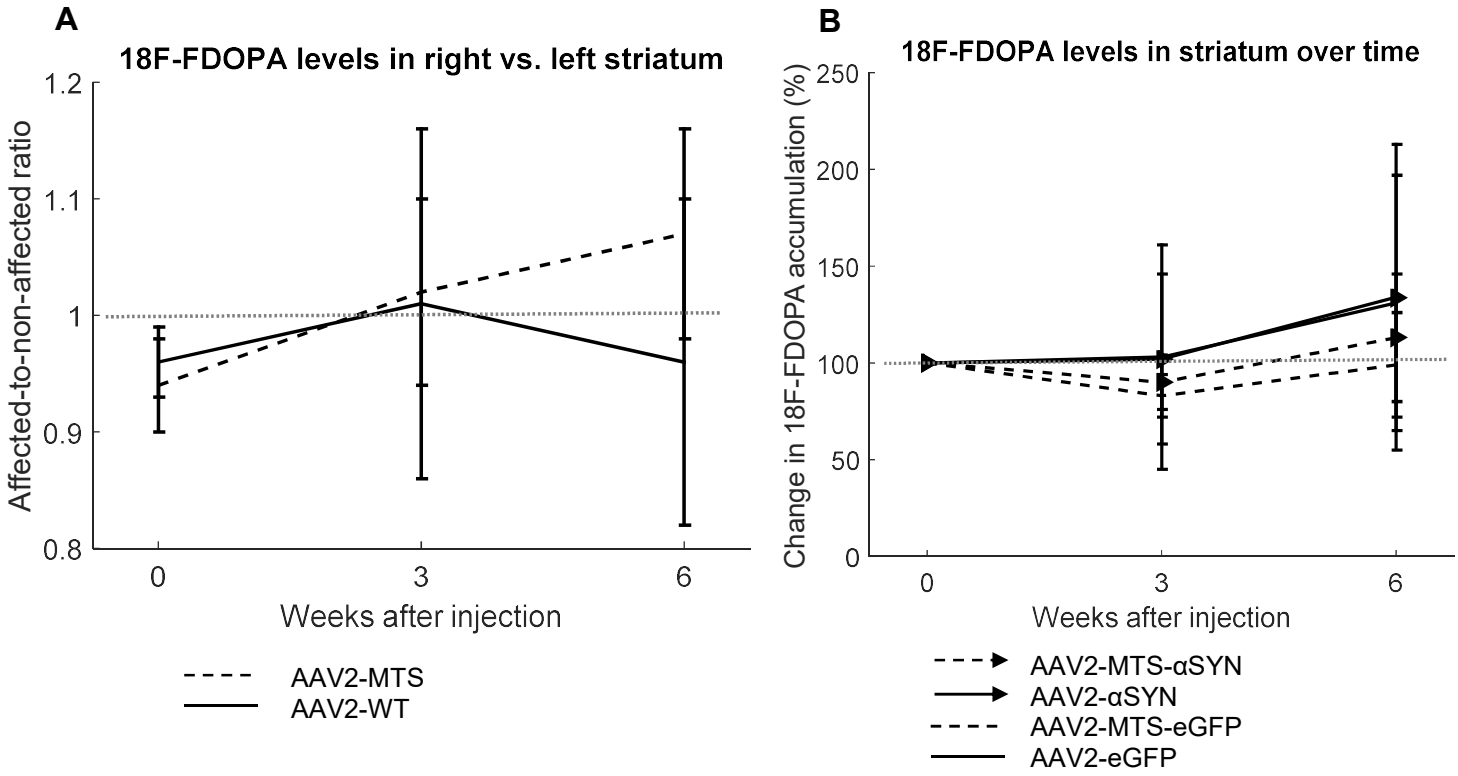

Figure 1. ^{18}F-FDOPA PET-imaging analysis. Functional dopaminergic activity was determined by standardizing to % ID and extracting tracer uptake values at week 3 and week 6 post-injection. No significant changes in tracer uptake following vector injection (normalized to baseline measurements, panel B). No significant three-way-interaction effect between time and hemisphere (panel A), and viral constructs AAV2-MTS (n = 7) and AAV2 (n = 6). Data are presented as the mean ± SD. AAV2 = adeno-associated virus serotype 2; MTS = mitochondrial targeting signal; WT = wild type; αSYN = alpha-synuclein; eGFP = enhanced green fluorescent protein.

^{11}C-PBR28 PET-imaging

One rat was excluded from analysis due to low quality of the scan at baseline. All animals exhibited a significant increase in striatal ^{11}C-PBR28 SUVs over time, $F(2, 20) = 4.8$, $p = .02$. However, differences between the cytosolic and mitochondrial targeting a-syn vectors at week 3 (.51 ± .13 vs. .5 ± .08) and week 6 (.59 ± .05 vs. .59 ± .12) were almost non-existent, $F(2, 20) = .05$, $p = .95$ (Fig. 2B). Although all viruses were associated with an overall gain in ^{11}C-PBR28 uptake over time, average SUV of the a-syn viruses exhibited a faster increase compared to the eGFP viruses. Larger differences between baseline values, week 3 and week 6 were found with the a-syn viruses than with the control viruses, $F(2, 20) = 9.12$, $p = .002$. This effect was especially apparent at week 3 when the SUV between baseline values and week 3 differed by .02 for eGFP vs. .05 for the a-syn viruses. However, differences between the cytosolic and mitochondrial targeting vectors were too small to reach significance, $F(2,$

20) = .37, p = .7 (Fig. 2A). Figure 3 shows the asymmetric distribution of ^{11}C-PBR28 uptake between the right and left striatum.

Table 2: *Mean and standard deviation of striatal SUVs by virus and timepoint.*

Virus	Pre-injection	Week 3	Week 6
AAV2-MTS-eGFP	.49 (SD .08)	.50 (SD .12)	.55 (SD .04)
AAV2-MTS-aSYN	.47 (SD .07)	.51 (SD .13)	.59 (SD .05)
AAV2-eGFP	.47 (SD .14)	.49 (SD .06)	.53 (SD .06)
AAV2-aSYN	.45 (SD .14)	.50 (SD .08)	.59 (SD .12)

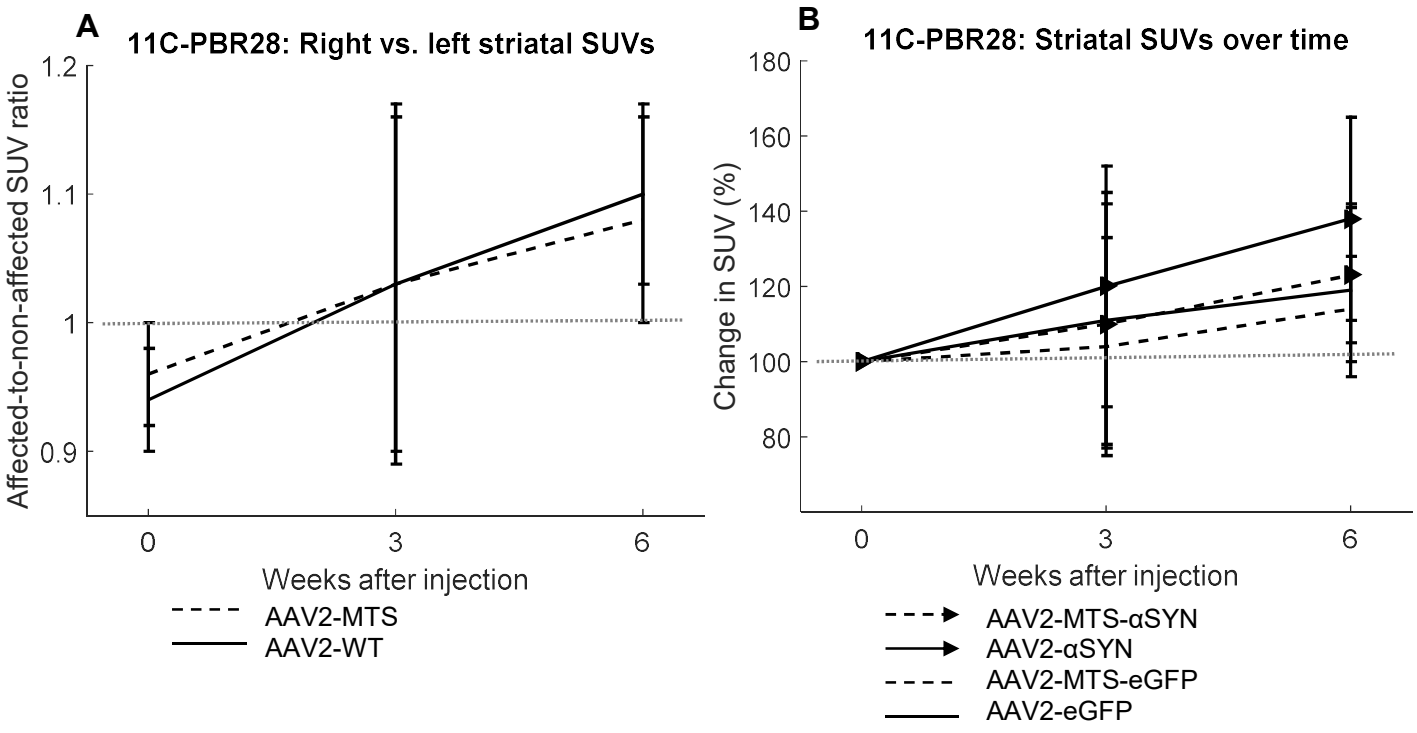

Figure 2. ^{11}C-PBR28 PET-imaging analysis. Neuroinflammation was determined by calculating the average SUV of a pre-defined brain region at week 3 and week 6 post-injection. There is a significant increase in SUV following α-syn overexpression (normalized to baseline measurements) (panel B), and a significant interaction effect between time and hemisphere (panel A). The ratio between left and right striatal SUVs increases over time, but independently of AAV2-MTS (n = 6) or AAV2 (n = 6) injection. Data are presented as the mean ± SD. AAV2 = adeno-associated virus serotype 2; MTS = mitochondrial targeting signal; WT = wild type; αSYN = alpha-synuclein; eGFP = enhanced green fluorescent protein.

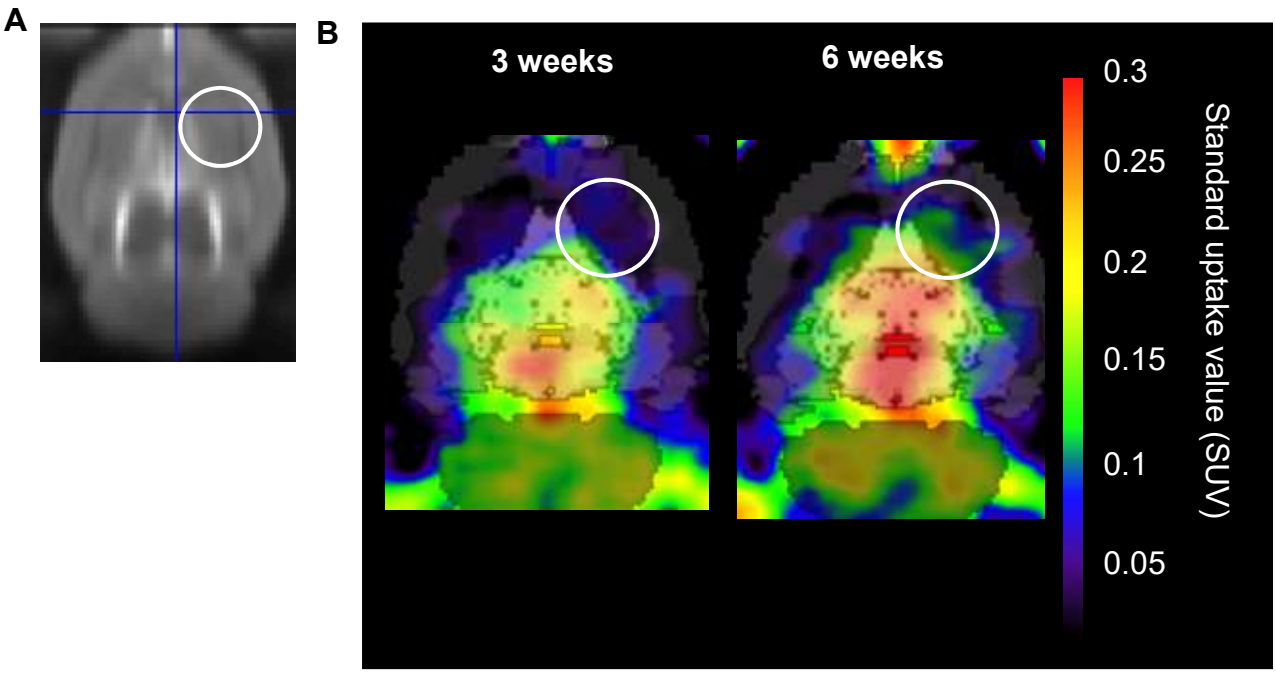

Figure 3. ^{11}C-PBR28 PET-imaging. Neuroinflammation was determined by calculating the average SUV of a pre-defined brain region at week 3 (B; left panel) and week 6 (B; right panel) post-injection, corrected to baseline measurements and averaged over all animals (n = 12). Panels depict transverse planes of the brain and are overlaid with the used brain atlas (Schwarz et al., 2006). The right striatum is encircled and an MRI template (Schwarz et al., 2006) is shown in figure A for anatomical references.

Cylinder test

Impaired forelimb activity did not change over the course of 6 weeks with $F(2, 22) = .13$, $p = .88$. Furthermore, there was no significant interaction effect between time and virus type with $F(2, 22) = .91$, $p = .42$.

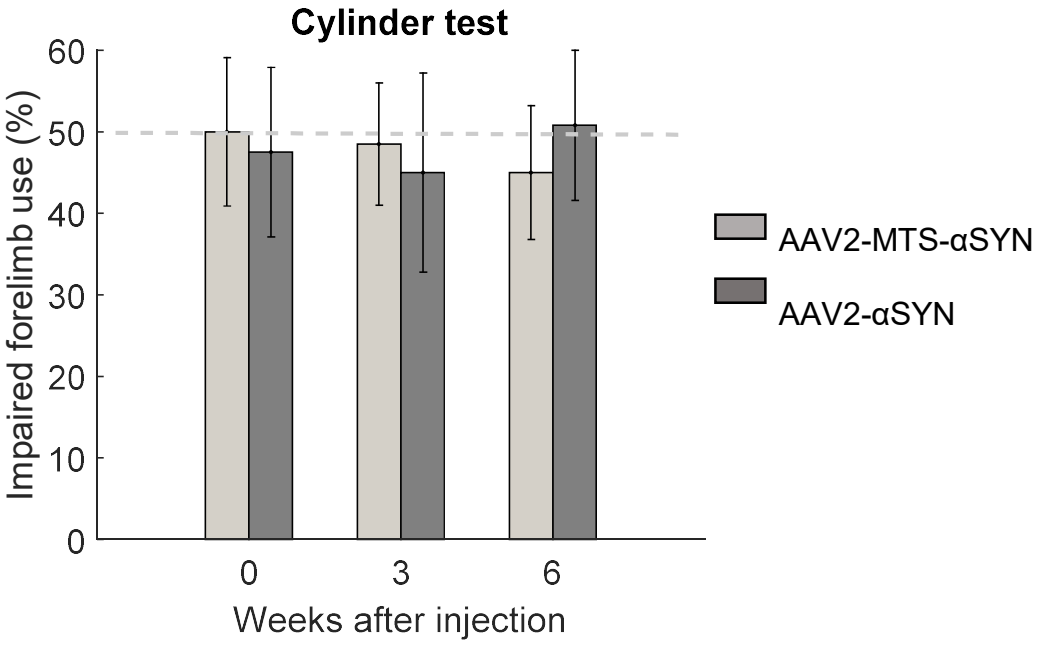

Figure 4. Behavioural analysis. Motor performance was examined using the cylinder test. Animals were tested at baseline, 3 and 6 weeks after AAV2-MTS (n = 7) or AAV2 (n = 6) injection. Data are presented as the mean ± SD. AAV2 = adeno-associated virus serotype 2; MTS = mitochondrial targeting signal; αSYN = alpha-synuclein.

Correlation analyses

Examination of linear correlations between PET parameters and behavioural data did not lead to significant associations between functional dopaminergic activity and motor performance (Fig. 5A), r = -0.13, p = 0.52, or the amount of striatal microglia activation and forelimb asymmetry (Fig. 5B), r = -0.04, p = 0.84. A random pattern of distribution can be seen in the figures, and the large variability between animals and time points is evident. However, there was a significant positive correlation between ^{18}F-FDOPA levels and ^{11}C-PBR28 uptake in the striatum of the α-syn injected side (Fig. 5C), r= 0.47, p=0.02. This association is apparent due to the increase in ^{18}F-FDOPA levels 6 weeks following injections which aligns with the increase in ^{11}C-PBR28 uptake. When only week 3 was considered, a meaningful relationship between both parameters seemed to be absent, r= 0.39, p= 0.19.

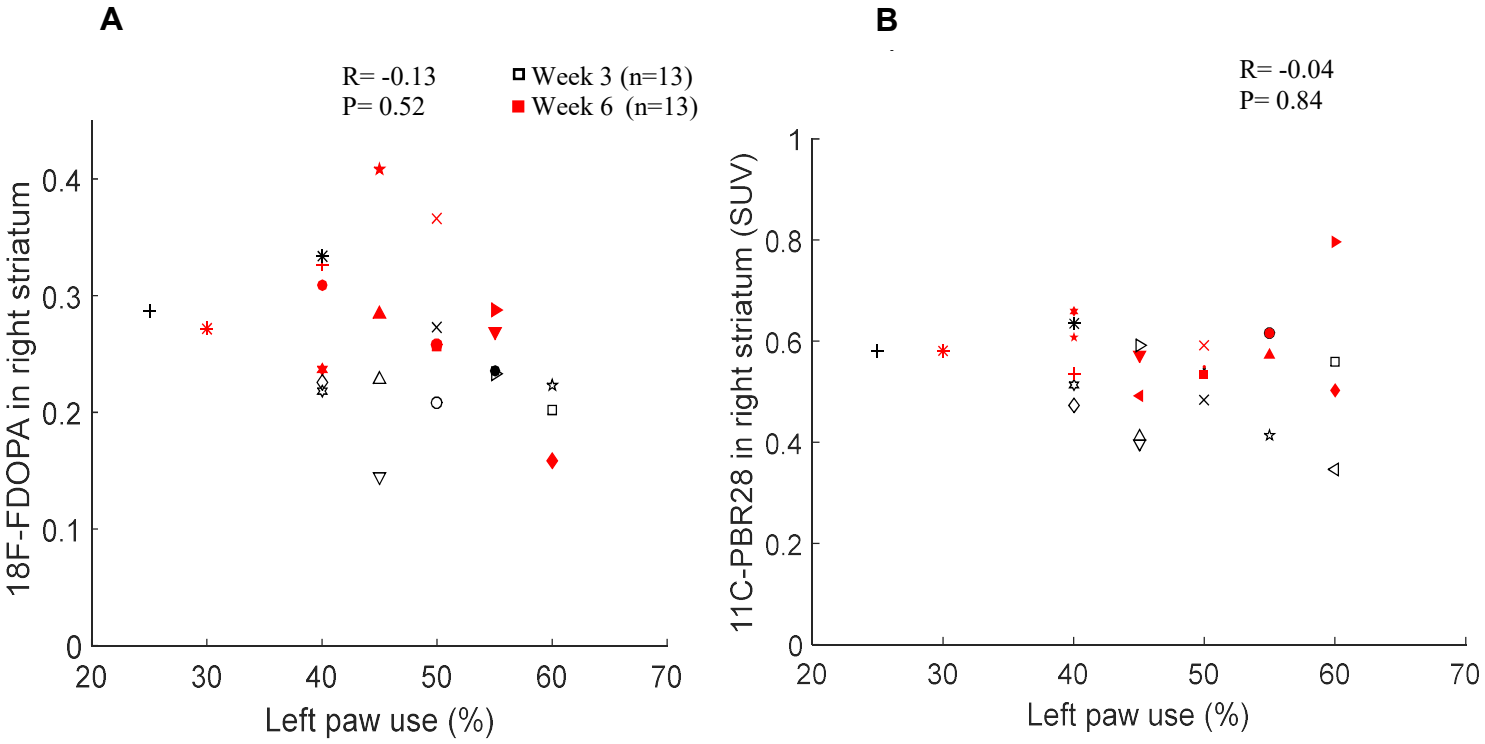

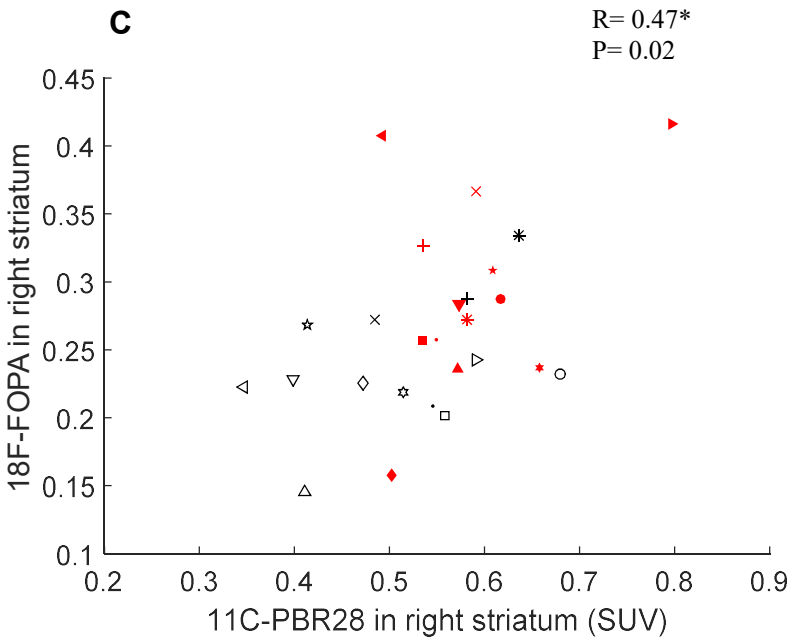

Figure 5. Scatter-plots showing the correlation between ^{18}F-FDOPA (panel A), ^{11}C-PBR28 (panel B) PET data and motor performance in the cylinder test. Every animal is labelled by a different symbol. Black outlined symbols represent measurements at week 3and red filled symbols represent measurements at week 6. Panel C shows the correlation between both PET parameters. Pearson correlation coefficient (r) and p values were calculated.

Discussion

The present study aimed to validate a novel, mitochondrial targeted α-syn overexpression model which was previously shown to successfully induce dopaminergic cell death *in vitro (Ganjam & Culmsee, personal communication)*. In this study, cytosolic targeted α-syn overexpression was compared to mitochondrial targeted α-syn overexpression *in vivo* by means of longitudinal microPET-imaging and behavioural testing. In contrast to previous studies, we adopted a within-subjects design in which animals received the α-syn overexpressing virus and an eGFP expressing control virus in the right and left SN, respectively. We expected to see the same temporal pattern of dopaminergic neurodegeneration *in vivo* as preliminary *in vitro* data indicated. Thus, dopaminergic neurons were hypothesized to degenerate faster when AAV2-MTS-αSYN had been injected compared to rats with the AAV2-αSYN virus. As such, impaired forelimb activity was expected to decline faster in the mitochondrial targeting compared to the cytosolic targeting vector.

Interestingly, current data does not show any significant differences between the control and α-syn side at 3 or 6 weeks post-injection regarding functional dopamine activity in the striatum. In line with the ^{18}F-FDOPA imaging data, there is no significant decrease in impaired forelimb activity over time. These results may indicate several possible issues in our

experimental design; (1) the eGFP virus might not serve as a reliable control vector and causes a similar amount of neuronal damage as the α-syn virus. In this way, no significant changes in the right-to-left ratio of striatal dopamine can be detected. Whether dopamine levels in the left and right striatum decrease equally over time should therefore be investigated further using a voxel-based analysis approach. However, the fact that preliminary *in vitro* data does not demonstrate overt neural injury by the eGFP vector renders this explanation unlikely. (2) Issues with tomographic image pre-processing such as image co-registration might counteract the ability to detect significant differences between hemispheres, especially when changes and/or regions of interest are small. Furthermore, PD is characterized by a delay in the appearance of motor symptoms as they appear only after a substantial decrease in striatal nerve terminals (i.e., 70–80%) and nigral cell bodies (i.e., 50–60%) (Bezard et al., 2003). Compensation mechanisms might therefore serve as an explanation for the lack of behavioural effects despite a possible onset of dopaminergic neurodegeneration too insignificant to be detected by PET imaging. (3) Although the current research is largely based on Decressac et al. (2012), there are mentionable differences between studies. For example, while Decressac and his co-workers used a combination of an AAV serotype 2 (i.e., the Inverted Terminal Repeat (ITR) sequences) and an AAV serotype 6 (i.e., the capsid proteins), current vectors were fully embedded in an AAV serotype 2. As such, differences in the temporal expression of pathology between studies are not unlikely. The AAV2 model might take longer to result in dopaminergic cell loss and associated behavioural deficits. Indeed, St Martin and her colleagues (2007) validated an AAV2 model for the targeted overexpression of α-syn in dopamine neurons of the SN in mice. Although the authors did not include any behavioural measures, TH-positive cell loss significantly differed between α-syn injected and control animals only at 24 weeks post-transduction. However, viral expression was abundant at 4 weeks suggesting that transduction efficiency is not substantially different from Decressac et al.'s (2012) AAV6/2 model. Previous reports of a significant loss in dopaminergic terminal density in the striatum could not be confirmed by St Martin and her colleagues (2007). This suggests that the absence of any differences between the left and right striatum in ^{18}F-FDOPA imaging does not necessarily indicate a complete lack of dopaminergic cell loss, or α-syn overexpression. Only after immunohistochemistry is performed, in which the presence of TH+ cells, α-syn and eGFP is checked, will we be able to make further inferences about the fitness of the current *in vivo* model.

Although no particular assumptions about the effects of α-syn overexpression on microglia could be made, we expected to see a time-dependent increase in microglia

activation in both virus groups. In addition, a higher amount of, and faster increase in microglia activation on the α-syn injected side compared to the eGFP injected side was predicted. In line with this assumption, there is a significant increase at week 3 compared to baseline values in the right-to-left ratio regarding the binding of the PET ligand ^{11}C-PBR28. Thus, α-syn overexpression elicits a higher activation of the brain's resident immune cells compared to the control side. Similar to week 3, week 6 post-injection is associated with a substantial increase in neuroinflammation compared to baseline measurements, but does not seem to diverge considerably from week 3 indicating a primarily early microglial response. However, due to problematic image co-registration and the use of multiple software, results need to be interpreted with caution. Also, the large variation between animals and the increase in overall neuroinflammation (e.g., cortex, cerebellum) indicates a possible influence of yet still unknown factors.

It is hypothesized that in PD, microglia activation is associated with the secretion of pro-inflammatory cytokines increasing the risk of neural injury. Using the same approach as St Martin et al. (2007), Theodore et al. (2008) have shown that CD68-positive microglia increase in numbers after targeted α-syn overexpression in the SN at 4 weeks post-transduction. The number of phagocytic microglia was shown to level off in the following 8 weeks suggesting a peak in microglia activation 3 to 5 weeks which is in accordance with our current results. Binding of neuroinflammatory PET ligands such as ^{3}H-PK11195 correlates with the abundance of CD68-positive macrophages (Venneti et al., 2009) implicating that our ^{11}C-PBR28 data can be aligned to the amount of phagocytic microglia. Additionally, Theodore et al. (2008) demonstrate elevated levels of pro-inflammatory cytokines such as IL-1 and TNF 2 weeks after viral transduction. Thus, the neuroinflammatory response is early despite the absence of dopaminergic neurodegeneration, and without the immediate consequence of dopaminergic cell loss. Ideally, the current study is prolonged and animals are tested over a larger longitudinal span. Furthermore, histological assessment of the brains is necessary to confirm viral expression, an elevated presence of α-syn in the SN extending to the striatum, and TH+ neuronal death.

Increased microglia activation might also have a neuroprotective effect on the dopaminergic system in the first weeks after viral transduction by taking up extracellular α-syn released from neighbouring dopamine neurons (Rey et al., 2013). Especially when transduction is not 100% successful and transcription rates of the α-syn encoding gene are low, microglia clearance of α-syn serves as a possible explanation of the absent decline in striatal dopamine. A comprehensive review by Hirsch et al. (2012) explains that dying

catecholaminergic neurons release neuromelanin into the extracellular space which is then taken up by surrounding microglia. Neuromelanin induces microglia activation leading to the generation of reactive species and the secretion of pro-inflammatory mediators suggesting that neural injury precedes neuroinflammatory reactions. However, whether the neuroinflammatory response occurs before PD-related dopaminergic cell loss is still debated in the literature. Rey et al. (2013) have shown that 72 hours after neuronal uptake of previously introduced normal and abnormal α-syn, a large portion of the added proteins appeared in surrounding activated microglia. Hence, internalization and the clearance of extracellular α-syn by microglia seems more likely providing further support for the present findings of a neuroinflammatory reaction before overt dopaminergic neuronal death. Similar to the present study, Chung et al. (2009) overexpressed a mutant type of α-syn (i.e., A53T) under the control of the synapsin gene promoter using an AAV2 vector in rats. In line with our current results, the authors show a pro-inflammatory response in the striatum before dopaminergic cell death. Furthermore, striatal dopamine loss was not observed at week 4 despite the presence of degenerative changes in striatal nerve terminals.

Apart from microglial activation, abnormal α-syn serves as a prime suspect for the activation of the adaptive immune system. Aberrant α-syn is thought to serve as the antigenic trigger for the activation of peripheral CD4- and CD8-positive lymphocytes. Indeed, lymphocytic infiltration in the SN and striatum has previously been established in post-mortem brains of PD patients (Hirsch et al., 2012). Harms and colleagues (2013) determined elevated expression levels of the major histocompatibility complex class II (MHC II) protein by microglia when α-syn is overexpressed *in vivo*. MHC II expression is restricted to antigen-presenting cells and serves as a crucial step in the cellular immune response, entailing the presentation of peptide antigens to CD4+ lymphocytes. Treatment of microglia with abnormal α-syn seems to induce antigen processing and presentation activity by microglia resulting in CD4+ cell proliferation and cytokine secretion (Harms et al., 2013) that may further contribute to dopaminergic neurodegeneration. Indeed, the same authors show that dopamine producing neurons in the SN express MHC class I after activation by pro-inflammatory mediators released from microglia. As a result, CD8+ T cells kill dopaminergic neurons that present the rightful combination of MHC class I and α-syn peptide. The absence of microglial activation and neuronal death in the SN of MHC II knock-out animals at 6 months post-transduction of the α-syn overexpressing viral vector (Harms et al., 2013) provides further support for the prominent role of the adaptive immune system in neuroinflammatory driven neurodegeneration.

Interestingly, neuroinflammation and dopamine levels seem to share a positive association. According to previous reports however, one would predict a high amount of neuroinflammation when dopamine levels are low. As previously discussed, a higher amount of microglial activation might go in parallel with insignificant changes in striatal dopamine levels. Thus, despite the presence of neuroinflammation, functional dopamine activity does not decline over time, but rather seems to rise after 3 weeks post-injection (although insufficient to reach significance).

Current results contrast with our hypothesis that mitochondrial targeting of a-syn overexpression leads to a faster and more aggressive PD phenotype. Present findings were virus-independent suggesting no differential effects between mitochondrial and cytosolic targeting vectors regarding neuroinflammation, striatal dopamine levels and motor impairment. However, a large amount of evidence points towards a prominent role of mitochondrial dysfunctions due to α-syn overexpression or abnormality. As such, current results should not lead to the full rejection of our hypotheses but rather form the basis for new experiments to further establish mitochondrial targeting of α-syn overexpression *in vivo*. A common characteristic of α-syn is the protein's natural occurring co-localization with the mitochondria, which is not restricted to α-syn positive neurons in the ventral midbrain (Li et al., 2007). In line with this, Devi et al. (2008) show that the N-terminus of the α-syn protein comprises a cryptic mitochondrial targeting sequence leading to a 16.5 % distribution of α-syn to the mitochondria (depending on proteolytic processing). This suggests that the mitochondria represent a natural target of the protein under normal circumstances. Thus, mitochondrial dysfunctions due to mitochondrial accumulation of α-syn forms a very likely consequence. The same authors found evidence for the association of α-syn with the inner membrane of the organelles supporting previous hypotheses that in PD, α-syn might interfere with mitochondrial complex I (Devi et al., 2008).

In conclusion, the current study is inconclusive regarding the differences in functional dopamine activity and neuroinflammation between cytosolic and mitochondrial targeting of α-syn overexpression *in vivo*. The lack of an asymmetric effect in both ^{18}F-FDOPA and behavioural data indicates possible flaws within the current experiment; (1) a viral effectivity insufficient to induce dopaminergic neurodegeneration at 6 weeks post-injection, (2) wrong targeting of viral injections, and/or (3) incorrect tomographic image processing. However, the presence of (widespread) neuroinflammation suggests a successful manipulation of microglia activation. Whether it results from α-syn overexpression or other factors has yet to be determined by immunohistochemistry.

References

Bartels, A. L., Willemsen, A. T. M., Doorduin, J., de Vries, E. F. J., Dierckx, R. A., & Leenders, K. L. (2010). [C-11]-PK11195 PET: Quantification of neuroinflammation and a monitor of anti-inflammatory treatment in Parkinson's disease. *Parkinsonism & Related Disorders, 16(1)*, 57 59. DOI: 10.1016/j.parkreldis.2009.05.005.

Beal, M. F. (2003). Mitochondria, Oxidative damage, and inflammation in parkinson's disease. *Ann. N. Y. Acad. Sci, 991*, 120-131.

Bender, A., Desplats, P., Spencer, B., Rockenstein, E., Adame, A., Elstner, M., Laub, C., Mueller, S., Koob, A. O., Mante, M., Pham, E., Klopstock, T., & Masliah, E. (2013). TOM40 Mediates Mitochondrial Dysfunction Induced by α-Synuclein Accumulation in Parkinson's Disease. *PLoS One, 8*(4), e62277.

Bendor J., Logan, T., & Edwards, R. H. (2013). The Function of alpha-Synuclein. *Neuron, 79(6)*. DOI: 10.1016/j.neuron.2013.09.004.

Bernis, M. E., Babila, J. T., Breid, S., Wüsten, K. A., Wüllner, U., & Tamgüney, G. (2015). Prion-like propagation of human brain-derived alpha-synuclein in transgenic mice expressing human wild-type alpha-synulcein. *Acta Neuropathologica Communications, 3*(75). DOI: 10.1186/s40478-015-0254-7.

Bezard, E., Gross, C. E., & Brotchie, J. M. (2003). Presymptomatic compensation in Parkinson's disease is not dopamine-mediated. Trends in Neurosciences, 4, 215-221.

Braak, H., de Vos, R. A., Bohl, J., & Del Tredici, K. (2006). Gastric α-synuclein immunoreactive inclusions in Meissner's and Auerbach's plexuses in cases staged for Parkinson's disease related brain pathology. *Neuroscience Letters, 396*, 67–72. DOI: 10.1016/j.neulet.2005.11.012.

Braak, H., Del Tredici, K., Rüb, U., de Vos, R. A., Jansen Steur, E. N., & Braak, E. (2003). Staging of brain pathology related to sporadic Parkinson's disease. *Neurobiology of Aging, 24*, 197–211.

Bernheimer, H., Birkmayer, W., Hornykiewicz, O., Jellinger, K., & Seitelberger, F. (1973). Brain dopamine and the syndromes of Parkinson and Huntington. Clinical, morphological and neurochemical correlations. *Journal of the Neurological Sciences, 20*, 415-455.

Burns, R. S., LeWitt, P. A., Ebert, M. H., Pakkenberg, H., & Kopin, I. J. (1985). The clinical syndrome of striatal dopamine deficiency. Parkinsonism induced by 1-methyl-4-phenyl 1,2,3,6-tetrahydropyridine (MPTP). *The New England Journal of Medicine, 312*, 1418–1421. DOI: 10.1056/NEJM198505303122203

Cannon, J. R., Tapias, V., Na, H. M., Honick, A. S., Drolet, R. E., & Greenamyre, J. T. (2009). A highly reproducible rotenone model of Parkinson's disease. *Neuriobiology of Disease, 34*(2), 279-290. DOI: 10.1016/j.nbd.2009.01.016.

Chung, C. Y., Koprich, J. B., Siddiqi, H., & Isacson, O. (2009). Dynamic Changes in Presynpatic and Axonal Transport Proteins Combined with Striatal Neuroinflammation Precede Dopaminergic Neuronal Loss in a Rat Model of AAV α Synucleinopathy. *Journal of Neuroscience, 29*(11), 3365-3373. DOI: 10.1523/JNEUROSCI.5427-08.2009.

Campbell, B. C., Li, Q. X., Cluvenor, J. G., Jäkälä, P., Cappai, R., Beyreuther, K., Masters, C. L., McLean, C. A. (2000). Accumulation of insoluble alpha-synuclein in dementia with Lewy bodies. *Neurobiology of Disease, 7(3),* 192-200. DOI: 10.1006/nbdi.2000.0286.

Croisier, E., Moran, L. B., Dexter, D. T., Pearce, R. K., & Graeber, M. B. (2005). Microglial inflammation in the parkinsonian substantia nigra: relationship to alpha-synuclein deposition. *Journal of Neuroinflammation, 2(*14*)*.

Dauer, W. & Przedborski, S. (2003). Parkinson's Disease: Mechanisms and Models. *Neuron, 39(6),* 889-909. DOI: 10.1016/S0896-6273(03)00568-3.

Dauer, W., Kholodilov, N., Vila, M., Trillat, A., Goodchild, R., Larsen, K. E., Staal, R., Tieu, K., Schmitz, Y., Yuan, C. A., Rocha, M., Jackson-Lewis, V., Hersch, S., Sulzer, D., Przedborski, S., Burke, R., & Hen, R. (2002). Resistance of α-synuclein null mice to the parkinsonian neurotoxin MPTP. *PNAS, 99*(22), 14524-14529. DOI: 10.1073/pnas.172514599.

Decressac, M., Ulusoy, A., Mattsson, M., Georgievska, B., Romero-Ramos, M., Kirik, D., & Bjorklund, A. (2011). GDNF fails to exert neuroprotection in a rat a-synuclein model of Parkinson's disease. *Brain, 134*, 2302–2311. DOI: 10.1093/brain/awr149.

Decressac, M., Mattsson, B., Lundblad, M., Weikop, P., & Björklund, A. (2012). Progressive neurodegenerative and behavioural changes induced by AAV-mediated overexpression of alpha synuclein in midbrain dopamine neurons. *Neurobiology of Disease, 45*, 939-953. DOI: 10.1016/j.nbd.2011.12.013.

Devi, L., Raghavendran, V., Prabhu, B. M., Avadhani, N. G., & Anandatheerthavarada, H. K. (2008). Mitochondrial import and accumulation of alpha-synuclein impair complex I in human dopaminergic neuronal cultures and Parkinson disease brain. *Journal of Biological Chemistry, 283*, 9089-9100.

Dheen, S. T., Kaur, C., & Ling, E. A. (2007). Microglial activation and its implications in the brain diseases. *Current Medicinal Chemistry, 14,* 1189–1197.

Garcia, D. V., Casteels, C., Schwarz, A. J., Dierckx, R. A. J. O., Koole, M., & Doorduin, J. (2015). A Standardized Method for the Construction of Tracer Specific PET and SPECT Rat Brain Templates: Validation and Implementation of a Toolbox. *PLOS ONE, 10*(11), e0143900. DOI: 10.1371/journal.pone.0143900.

Gao, H., Kotzbauer, P. T., Uryu, K., Leight, S., Trojanowski, J. Q., & Lee, V. M. (2008). Neuroinflammation and Oxidation/Nitration of α-Synuclein Linked to Dopaminergic Neurodegeneration. *Journal of Neuroscience, 28*(30)*,* 7687-7698. DOI: 10.1523/JNEUROSCI.0143-07.2008.

Giasson, B. I., Duda, J. E., Murray, I. V., Chen, Q., Souza, J. M., Hurtig, H. I., Ischiropoulos, H., Trojanowski,J. Q., & Lee, V. M. (2000). Oxidative damage linked to neurodegeneration by selective alpha-synuclein nitration in synucleinopathy lesions. *Science, 290*, 985-989. DOI: 10.1126/science.290.5493.985.

Harms, A. S., Cao, S., Rowse, A. L., Thome, A. D., Li, X., Mangieri, L. R., Cron, R. Q., Shacka, J. J., Raman, C., & Standaert, D. G. (2013). MHCII is required for α -synuclein-induced activation of microglia, CD4 T cell proliferation, and dopaminergic neurodegeneration. *Journal of Neuroscience, 33*(23), 9592–9600. DOI:10.1523/JNEUROSCI.5610-12.2013.

Hirsch, E. C., Vyas, S., & Hunota, S. (2012). Neuroinflammation in Parkinson's disease. *Parkinsonism and Related Disorders, 18*, 210-212.

Holmqvist, S., Chutna, O., Bousset, L., Aldrin-Kirk, P., Li, W., Björklund, T., Wang, Z., Roybon, L., Melki, R., & Li, J. (2014). Direct evidence of Parkinson pathology spread from the gastrointestinal tract to the brain in rats. *Acta Neuropathologica, 128*, 805-820. DOI: 10.1007/s00401-014-1343-6.

Hsu, L. J., Sagara, Y., Arroyo, A., Rockenstein, E., Sisk, A., Mallory, M., Wrong, J., Takenouchi, T., Hashimoto, M., & Masliah, E. (2000). Alpha-Synuclein Promotes Mitochondrial Deficit and Oxidative Stress. *The American Journal of Pathology*, *157*(2), 401–410. DOI: 10.1016/S0002-9440(10)64553-1.

Ibanez, P. et al. (2004). Causal relation between alpha-synuclein gene duplication and familial Parkinson's disease. *Lancet, 364*, 1169–1171. DOI: 10.1016/S0140-6736(04)17104-3.

Imaizumi, M., Briard, E., Zoghbi, S. S., Gourley, J. P., Hong, J., Fujimura, Y., Pike, V. W., Innis, R. B., & Fujita, M. (2008). Brain and Whole-body Imaging in Nonhuman Primates of [^{11}C]-

PBR28, a Promising PET Radioligand for Peripheral Benzodiazepine Receptors. *Neuroimage, 39*(3), 1289-1298. DOI: 10.1016/j.neuroimage.2007.09.063.

Jeon, B. S., Jackson-Lewis, V., & Burke, R. E. (1995). 6-hydroxydopamine lesion of the rat substantia nigra: Time course and morphology of cell death. *Neurodegeneration, 4*, 131-137.

Kirik, D., Rosenblad, C., Burger, C., Lundberg, C., Johansen, T. E., Muzyczka, N., Mandel, R. J., & Björklund, A. (2002). Parkinson-like neurodegeneration induced by targeted overexpression of alpha-synuclein in the nigrostriatal system. *Journal of Neuroscience, 22*, 2780–2791. DOI: 20026246.

Kügler, S., Kilic, E., & Bähr, M. (2003). Human synapsin 1 gene promoter confers highly neuron specific long-term transgene expression from an adenoviral vector in the adult rat brain depending on the transduced area. *Gene Therapy, 10*(4)*,* 337-347. DOI: 10.1038/sj.gt.3301905.

Kruger, R., Kuhn, W., Muller, T., Woitalla, D., Graeber, M., Kosel, S., Pzuntek, H., Epplen, J. T., Schols, L., & Riess, O. (1998). Ala30Pro mutation in the gene encoding alpha-synuclein in Parkinson's disease. *Nature Genetics, 18*, 107-108. DOI: 10.1038/ng0298-106.

Kyono, K., Takashima, T., Katayama, Y., Kawasaki, T., Zochi, R., Gouda, M., Kuwahara, Y., Takahashi, K., Wada, Y., Onoe, H., & Watanabe, Y. (2011). Use of [^{18}F]FDOPA-PET for in vivo evaluation of dopaminergic dysfunction in unilaterally 6-OHDA-lesioned rats. *European Journal of Nuclear Medicine and Molecular Imaging, 1*(25). DOI: 10.1186/2191-219X1-25.

Langston, J. W., Ballard, P., Tetrud, J. W., & Irwin, I. (1983). Chronic Parkinsonism in humans due to a product of meperidine-analog synthesis. *Science, 219*, 979–80.

Li, J., O, W., Li, W., Jiang, Z. G., & Ghanbari, H. A. (2013). Oxidative stress and neurodegenerative *disorders. International Journal of Molecular Sciences, 14*(12*),* 24438-24475. DOI: 10.3390/ijms141224438.

Li, W., Yang, R., Guo, J. C., Ren, H. M., Zha, X. L., Cheng, J. S., & Cai, D. F. (2007). Localization of alpha-synuclein to mitochondria within midbrain of mice. *Neuroreport, 18*, 1543-1546. DOI: 10.1097/WNR.0b013e3282f03db4.

Loening, A. M. & Gambhir, S. S. (2003). AMIDE: A Free Software Tool for Multimodality Medical Image Analysis. *Molecular Imaging, 2*(3), 131-137.

Matsuoka, Y., Vila, M., Lincoln, S., McCormack, A., Picciano, M., LaFrancois, J., Yu, X., Dickson, D., Langston, J. W., McGowan, E., Farrer, M., Hardy, J., Duff, K., Przedborski S., &
Di Monte, D. A. (2001). Lack of nigral pathology in transgenic mice expressing human alpha synuclein driven by the tyrosine hydroxylase promoter. *Neurobiology of Disease, 8*(3), 535 539. DOI: 10.1006/nbdi.2001.0392.

Parihar, M. S., Parihar, A., Fujita, M., Hashimoto, M., & Ghafourifar, P. (2008). Mitochondrial association of alpha-synuclein causes oxidative stress. *Cellular and Molecular Life Sciences, 65*, 1272-1284. DOI: 10.1007/s00018-008-7589-1.

Parihar, M. S., Parihar, A., Fujita, M., Hashimoto, M., & Ghafourifar, P. (2009). Alpha-synuclein overexpression and aggregation exacerbates impairment of mitochondrial functions by augmenting oxidative stress in human neuroblastoma cells. *The International Journal of Biochemistry & Cell Biology, 41*, 2015-2024. DOI: 10.1016/j.biocel.2009.05.008.

Perier, C., Tieu, K., Guégan, C., Caspersen, C., Jackson-Lewis, V., Carelli, V., Martinuzzi, A., Hirano, M., Przedborski, S., & Vila, M. (2005). Complex I deficiency primes Bax-dependent neuronal apoptosis through mitochondrial oxidative damage. *PNAS, 102*, 19126-19131. DOI: 10.1073/pnas.0508215102.

Perier, C., Bov, E. J., Dehay, B., Jackson-Lewis, V., Rabinovitch, P. S., Przedborski, S., & Vila, M. (2010). Apoptosis-inducing factor deficiency sensitizes dopaminergic neurons to parkinsonian neurotoxins. *Annals of Neurology, 68*, 184–192. DOI: 10.1002/ana.22034.

Polymeropoulos, M. H., Lavedan, C., Leroy, E., Ide, S. E., Deheija, A., Dutra, A., Pike, B., Root, H., Rubenstein, J., Boyer, R., Stenroos, E. S., Chandrasekharappa, S., Athanassiadou, A., Papapetropoulos, T., Johnson, W. G., Lazzarini, A. M., Duvoisin, R. C., Di Iorio, G., Golbe, L. I., & Nussbaum, R. L. (1997). Mutation in the alpha-synuclein gene identified in families with Parkinson's disease. *Science, 276*, 2045-2047.

Reish, H. E. A. & Standaert, D. G. (2015). Role of a-synuclein in inducing innate and adaptive immunity in Parkinson disease. *Journal of Parkinsons Disease, 5*(1), 1-19. DOI: 10.3233/JPD 140491.

Rey, N. L., Petit, G. H., Bousset, L., Melki, R., & Brundin, P. (2013). Transfer of human α-synuclein from the olfactory bulb to interconnected brain regions in mice. *Acta Neuropathologica*, 126(4), 555-573. DOI: 10.1007/s00401-013-1160-3.

Rockenstein, E., Nuber, S., Ovkerk, C. R., Ubhi, K., Mante, M., Patrick, C., Adame, A., Trejo Morales, M., Gerez, J., Picotti, P., Jensen, P. H., Campioni, S., Riek, R., Winkler, J., Gage, F. H., Winner, B., & Masliah, E. (2014). Accumulation of oligomer-prone α-synuclein exacerbates synaptic and neuronal degeneration in vivo. *Brain, 137,* 1496-1513. DOI: 10.1093/brain/awu057.

Sanchez-Guajardo, V., Febbraro, F., Kirik, D., & Romero-Ramos, M. (2010). Microglia acquire distinct activation profiles depending on the degree of alpha-synuclein neuropathology in a rAAV based model of Parkinson's disease. *PLoS One, 5*(1), e8784. DOI: 10.1371/journal.pone.0008784.

Schapira, A. H., Cooper, J. M., Dexter, D., Clark, J. B., Jenner, P., & Marsden, C. D. (1990). Mitochondrial complex I deficiency in Parkinson's disease. *Journal of Neurochemistry, 54*(3), 823-827.

Schapira, A. H. (2007). Mitochondrial dysfunction in Parkinson's disease. *Cell Death & Differentiation, 14*(7), 1261-1266. DOI: 10.1038/sj.cdd.4402160.

Schwarz, A. J., Danckaert, A., Reese, T., Gozzi, A., Paxinos, G., Watson, C., Merlo-Pich, E. V., & Bifone, A. (2006). A stereotaxic MRI template set for the rat brain with tissue class distribution maps and co-registered anatomical atlas: application to pharmalogical MRI. *Neuroimage, 32*(2), 538-550. DOI: 10.1016/j.neuroimage.2006.04.214.

Singleton, A. B., Farrer, M., Johnson, J., Singleton, A., Hague, S., Kachergus, J., Hulihan, M., Peuralinna, T., Dutra, A., Nussbaum, R., Lincoln, S., Crawley, A., Hanson, M., Maraganore, D., Adler, C., Cookson, M. R., Muenter, M., Baptista, M., Miller, D., Blancato, J., Hardy, J., & Gwinn-Hardy, K. (2003). alpha-Synuclein locus triplication causes Parkinson's disease. *Science, 302*, 841. DOI: 10.1126/science.1090278.

Spillantini, M. G., Schmidt, M. L., Lee, V. M., Trojanowski, J. Q., Jakes, R., & Goedert, M. (1997). A Synuclein in Lewy bodies. *Nature, 388*, 839–840. DOI: 10.1038/42166

Spinelli, K. J., Taylor, J. K., Osterberg, V. R., Churchill, M. J., Pollock, E., Moore, C., Meshul, C. K., & Unni, V. K. (2014). Presynaptic Alpha-Synuclein Aggregation in a Mouse Model of Parkinson' s Disease. *Journal of Neuroscience*, *34*(6), 2037–2050. DOI: 10.1523/JNEUROSCI.2581-13.2014.

St Martin, J. L., Klucken, J., Outeiro, T. F., Nguyen, P., Keller-McGandy, C., Cantuti-Castelvetri, I., Grammatopoulos, T. N., Standaert, D. G., Hyman, B. T., & McLean, P. J. (2007). Dopaminergic neuron loss and up-regulation of chaperone protein mRNA induced by targeted over-expression of alpha-synuclein in mouse substantia nigra. *Journal of Neurochemistry*, *100*(6), 1449–1457. DOI: 10.1111/j.1471-4159.2006.04310.x .

Taylor, J. M., Main, B. S., Crack, P. J. (2013). Neuroinflammation and oxidative stress: Co-conspirators in the pathology of Parkinson's disease. *Neurochemistry International, 62*, 803 819. DOI:1 0.1016/j.neuint.2012.12.016.

Theodore, S., Cao, S., McLean, P. J., & Standeart, D. G. (2008). Targeted overexpression of human a synuclein triggers microglial activation and an adaptive immune response in a mouse model of Parkinson disease. *Journal of Neuropathology Experimental Neurology, 67*, 1149-1158.

Thomas, B & Beal, M. F. (2007). Parkinson's disease. *Human Molecular Genetics, 2*, 183-194. DOI: 10.1093/hmg/ddm159.

Tóth, M., Dooorduin, J., Häggkvist, J., Varrone, A., Amini, N., Halldin, C., & Gulyás, B. (2015). Positron Emission Tomography studies with [^{11}C]-PBR28 in the Healthy Rodent Brain: Validation SUV as an Outcome Measure of Neuroinflammation. *PLoS One, 10*(5), e0125917. DOI: 10.1371/journal.pone.0125917.

Ungerstedt, U. (1968). 6-Hydroxydopamine induced degeneration of central monoamine neurons. *European Journal of Pharmacology, 5,* 107–110.

Van der Perren, A., Toelen, J., Casteels, C., Macchi, F., Van Rompuy, A., Sarre, S., Casadei, N., Nuber, S., Himmelreich, U., Osorio Garcia, M., Michotte, Y., D'Hooge, R., Bormans, G., Van Laere, K., Gijsbers, R., Van den Haute, C., Debyser, Z., & Baekelandt, V. (2015). Longitudinal follow-up and characterization of a robust rat model for Parkinson's disease based on overexpression of alpha synuclein with adeno associated viral vectors. *Neurobiology of Ageing, 36,* 1543-1558. DOI: 10.1016/j.neurobiolaging.2014.11.015.

Venneti, S., Lopresti, B. J., Wang, G., Hamilton, R. L., Mathis, C. A., Klunk, W. E., Apte, U. M., & Wiley, C. A. (2009). PK11195 labels activated microglia in Alzheimer's diseaseand in vivo in a mouse model using PET. *Neurobiology of Aging, 30*(8), 1217-1226. DOI: 10.1016/j.neurobiolaging.2007.11.005.

Visanji, N. P., Brotchie, J. M., Kalia, L. V., Koprich, J. B., Tandon, A., Watts, J. C., & Lang, A. E. (2016). A-Synuclein-Based Animal Models of Parkinson's Disease: Challenges and Opportunities in a New Era. *Trends in Neurosciences, 39*(11). DOI: 10.1016/j.tins.2016.09.003.

Zhang, W., Wang, T., Pei, Z., Miller, D. S., Wu, X., Block, M. L., Wilson, B., Zhang, W., Zhou, Y., Hong, J. S., & Zhang, J. (2005). Aggregated alpha-synuclein activates microglia: a process leading to disease progression in Parkinson's disease. *FASEB Journal, 19*, 533–542. DOI: 10.1096/fj.04-2751com.

Appendix

Rat number	*Left striatum*	*Right striatum*	*Weight at surgery (gr)*	*Weight at week 3 (gr)*	*Weight at week 6 (gr)*
34	AAV2-MTS-eGFP	AAV2-MTS-aSYN	277	300	298
35	AAV2-MTS-eGFP	AAV2-MTS-aSYN	222	252	254
36	AAV2-MTS-eGFP	AAV2-MTS-aSYN	248	266	289
37	AAV2-WT-eGFP	AAV2-WT-aSYN	237	240	256
38	AAV2-MTS-eGFP	AAV2-MTS-aSYN	241	240	254
39	AAV2-MTS-eGFP	AAV2-MTS-aSYN	242	247	268
40	Died during surgery	Died during surgery	Died during surgery	Died during surgery	Died during surgery
41	AAV2-WT-eGFP	AAV2-WT-aSYN	253	268	282
42	AAV2-WT-eGFP	AAV2-WT-aSYN	243	258	270
43	Died during surgery	Died during surgery	Died during surgery	Died during surgery	Died during surgery
44	AAV2-WT-eGFP	AAV2-WT-aSYN	238	249	271
45	AAV2-MTS-eGFP	AAV2-MTS-aSYN	215	239	247
46	Died during surgery	Died during surgery	Died during surgery	Died during surgery	Died during surgery
47	AAV2-MTS-eGFP	AAV2-MTS-aSYN	222	237	249
48	AAV2-WT-eGFP	AAV2-WT-aSYN	225	244	261
49	AAV2-WT-eGFP	AAV2-WT-aSYN	212	233	241

Figure 6. Detailed overview of the performed injections and the animals' weight at the time of surgery, 3 and 6 weeks following injections.

Viruses

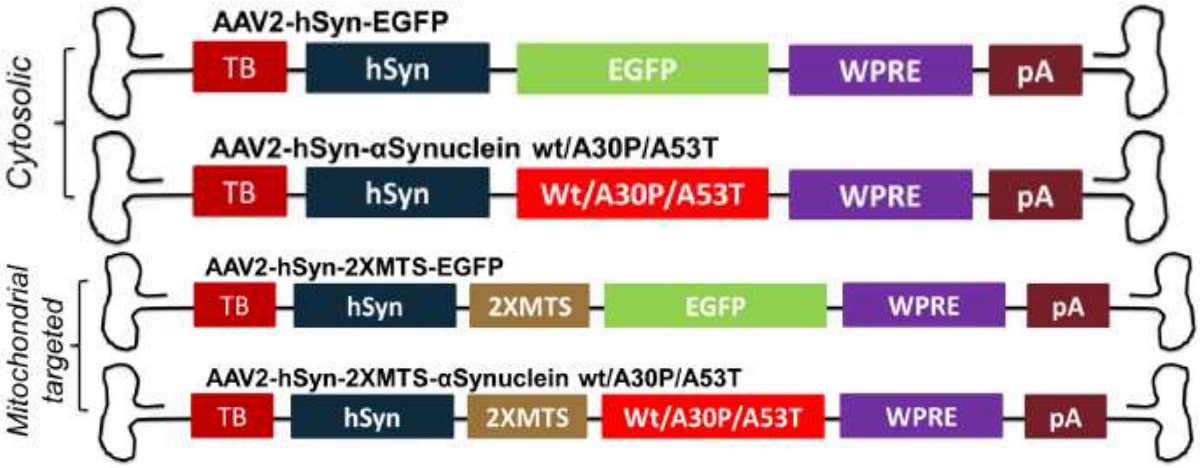

Figure 7. Viral genome expression cassettes. The cytosolic targeting a-syn vectors include the a-syn associated genes while the control vector possesses an eGFP cassette. This is the same for the mitochondrial targeting vectors. TB = Transcription blocker; hSyn = human Synapsin1 promoter; WPRE = woodchuck posttranscriptional regulatory element; pA = polyadenylation signal; 2XMTS = two times mitochondrial targeting signal sequence; A30P, A53T = mutant alpha-synucleins; WT = wild type.